Available online at www.sciencedirect.com
SCIENCE DIRECT®
Journal of Sound and Vibration 273 (2004) 695–711
JOURNAL OF SOUND AND VIBRATION
www.elsevier.com/locate/jsvi

Closed-loop non-linear control of an initially imperfect beam with non-collocated input

W. Lacarbonara[a,*], H. Yabuno[b]

[a] *Dipartimento di Ingegneria Strutturale e Geotecnica, University of Rome La Sapienza, via Eudossiana 18,00184 Rome, Italy*
[b] *Institute of Engineering Mechanics and Systems, University of Tsukuba, Tsukuba-City 305-8573, Japan*

Received 2 September 2002; accepted 8 May 2003

Abstract

A closed-loop non-linear control strategy to reduce the flexural vibrations of a hinged–hinged initially imperfect beam is investigated. The beam is subjected to a harmonic transverse excitation involved in a primary resonance of the first antisymmetric mode. A closed-loop symmetric control action—bending moments imparted by two piezoceramic actuators—although non-collocated, is designed to be non-orthogonal, in a non-linear sense, to the excited mode and be capable of exerting resonant beneficial damping effects onto it. The approximate responses of the controlled and uncontrolled beam are constructed by applying the method of multiple scales directly to the integral–partial differential equations of motion and boundary conditions. The frequency response curve governing the primary resonance of the uncontrolled system is compared with that obtained when the controller is in action. It is shown that, by exerting feasible control efforts, the response of the beam may be reduced by an order of magnitude and is stable in the overall frequency range in contrast with the uncontrolled large-amplitude responses which undergo jumps at the saddle-node bifurcations.

1. Introduction

Shallow structures such as shallow arches and shells are widely used in civil engineering (e.g., bridges) as well as in mechanical and aerospace applications, often employed as subcomponents of larger structures. It is well known that the presence of initial curvature induces quadratic internal forces which act along with cubic non-linear forces whose nature depends on the specific system with the associated boundary conditions. External resonant excitations may be sources of

*Corresponding author.
E-mail address: walter.lacarbonara@uniroma1.it (W. Lacarbonara).

0022-460X/$ - see front matter © 2003 Elsevier Ltd. All rights reserved.
doi:10.1016/j.jsv.2003.05.001

undesirable flexural vibrations. Among external resonances there are primary and secondary resonances (of the combination, sub-harmonic, and super-harmonic types) and parametric resonances [1].

The task of reducing the detrimental effects of resonant disturbances has been tackled employing a variety of approaches ranging from direct disturbance rejection via classical control theory techniques to the use of vibration absorbers attached to the main system as dedicated substructures. For example, a number of works have addressed both theoretically and experimentally the problem of controlling transverse oscillations in distributed-parameter systems by parametric-type control actions [2,3] or by coupling autoparametrically the system to an electronic circuit to exploit the saturation phenomenon due to a two-to-one internal resonance [4]. In Ref. [5] it was shown that a parametric resonance in a cantilever beam can be suppressed by attaching a pendulum absorber to the beam tip and exploiting the low static friction produced at its pivot. The friction acts to shift the unstable region (where the parametric resonance is activated) in the excitation amplitude-frequency plane. As an alternative to passive approaches, a closed-loop feedback method was developed theoretically and experimentally to stabilize the principal parametric resonance in a cantilever beam using a piezoceramic patch in Ref. [6]. By employing the method of multiple scales, it was shown that a velocity- and displacement-based linear feedback law possesses the ability to shift the unstable region so that the parametric resonance is suppressed.

In a recent paper [7], using the asymptotic perturbation method, the primary resonance of a cantilever beam under state feedback control with a time delay has been investigated. Analysis of the modulation equations of the amplitude and phase of the oscillator has indicated that vibration control can be performed with appropriate time delay and feedback gains.

A general methodology was proposed in Refs. [8,9] to design non-linear control schemes for open-loop resonance cancellation in discrete and distributed-parameter weakly non-linear systems by employing a perturbation approach. It was shown that a direct perturbation expansion of the system dynamics facilitates understanding of the mechanisms by which the non-linear actuator inputs may be used to suppress the resonant parts of the excitation. Depending on the specific system, different mechanisms for generating effective non-linear actuator actions can be exploited. Furthermore, when excitations and actuations are non-collocated (e.g., when the actuation has zero projection, in a linear sense, on the dynamics to be controlled), classical linear control techniques break down. On the contrary, perturbation expansions of the non-linear system dynamics indicate how, due to the inherent structural non-linearities, the non-linear controller action may be intelligently designed to cancel or reduce significantly the resonances.

To show the feasibility of the open-loop resonance-cancellation methodology, a control strategy was developed in Ref. [9] for a shallow arch excited by a longitudinal end-displacement which is parametrically resonant with the first antisymmetric mode and the control input is a transverse force at the midspan. The exploited mechanism was a sub-harmonic resonance of order one-half. In a previous work [10], similar concepts were employed to address non-collocated disturbances via non-linear actuator action in a pendulum-type crane architecture.

Lately, the open-loop non-linear vibration control method proposed in Ref. [9] has been implemented theoretically and experimentally in Ref. [11]. Therein, the principal parametric resonance has been stabilized in a magnetically levitated body using an actively actuated pendulum-type vibration device.

Nonetheless, during the transient phase or, in general, when the disturbance is subjected to some changes, open-loop schemes show their inherent limitations. This is the basic motivation for investigating, in the present paper, a closed-loop non-linear strategy to control a hinged–hinged initially imperfect beam whose first antisymmetric mode is excited via a primary resonance disturbance.

The symmetric control action—bending moments imparted by symmetrically distributed piezoceramic actuators—is non-collocated as it is orthogonal, in a linear sense, to the externally excited mode. The closed-loop control input is designed so as to be capable of reducing the beam flexural vibrations at resonance with feasible control efforts. Proving that a non-linear controller with a symmetric input can reduce also antisymmetric vibrations entails the expansion of the control capabilities by exploitation of the structural non-linearities with respect to the linear theory. The same controller designed primarily to reduce symmetric oscillations may be used to reduce antisymmetric vibrations which, under some excitation conditions, can be excited simultaneously with symmetric vibrations. Because the fact that a symmetric input has control authority over symmetric vibrations is trivial, in the present study, the effectiveness of the symmetric non-linear input in reducing antisymmetric vibrations is analytically validated.

Mixed-mode (symmetric/antisymmetric) vibrations occur, e.g., in suspension bridges where usually the lowest mode is antisymmetric and is close to the first symmetric mode. Further, long-span bridges are usually designed with a moderate initial rise; however, the non-linear restoring forces are mainly generated by the supporting cables other than by the beam centerline stretching (as it occurs in beams with immovable hinges). Moreover, typical earthquakes possess most of the energy around the lowest natural frequencies. Because the seismically induced support motions are not, generally, in phase (for long-span bridges), they may excite also the first antisymmetric mode.

The objective of this work is to provide a proof of concept for the general non-linear control methodology. In this perspective, it is not claimed, for example, that piezoceramic patches are viable actuators for long-span bridges. However, it is not impractical, for truss bridges, to conceive inclusion of intermediate strain-actuated active trusses that can supply equivalent bending moments along the beam span, similarly to the piezoceramic action.

In Section 2, the equations of motion of the initially imperfect beam including the piezoceramic actuators are presented in dimensional and non-dimensional forms. In Section 3, the derivation of the closed-loop control strategy via perturbation treatment of the governing equations is discussed. The features of the system uncontrolled and controlled responses are also discussed in detail. In Section 4, the control performance is investigated. Finally, in Section 5, some concluding remarks are presented.

2. Problem formulation and equations of motion

The local planar flexural dynamics of a hinged–hinged initially imperfect homogeneous Euler–Bernoulli beam around the initial configuration $\hat{\psi}$ (Fig. 1) are governed by the following equation in dimensional form [12]:

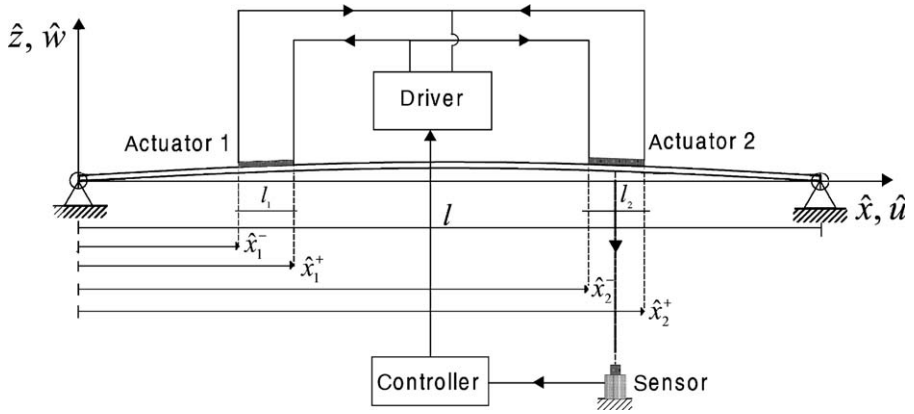

Fig. 1. Schematics of the beam with the control architecture.

$$\rho_b A_b \frac{\partial^2 \hat{w}}{\partial \hat{t}^2} + E_b I_b \frac{\partial^4 \hat{w}}{\partial \hat{x}^4} - \frac{E_b A_b}{\ell} \frac{\mathrm{d}^2 \hat{\psi}}{\mathrm{d}\hat{x}^2} \int_0^\ell \frac{\mathrm{d}\hat{\psi}}{\mathrm{d}\hat{x}} \frac{\partial \hat{w}}{\partial \hat{x}} \mathrm{d}\hat{x} - \frac{E_b A_b}{\ell} \frac{\partial^2 \hat{w}}{\partial \hat{x}^2} \int_0^\ell \frac{\mathrm{d}\hat{\psi}}{\mathrm{d}\hat{x}} \frac{\partial \hat{w}}{\partial \hat{x}} \mathrm{d}\hat{x} - \frac{E_b A_b}{2\ell} \frac{\mathrm{d}^2 \hat{\psi}}{\mathrm{d}\hat{x}^2} \int_0^\ell \left(\frac{\partial \hat{w}}{\partial \hat{x}} \right)^2 \mathrm{d}\hat{x} - \frac{E_b A_b}{2\ell} \frac{\partial^2 \hat{w}}{\partial \hat{x}^2} \int_0^\ell \left(\frac{\partial \hat{w}}{\partial \hat{x}} \right)^2 \mathrm{d}\hat{x} = \hat{F}(\hat{x}, \hat{t}) - \hat{c} \frac{\partial \hat{w}}{\partial \hat{t}} + \hat{U}(\hat{x}, \hat{t}), \tag{1}$$

with boundary conditions

$$\hat{w} = 0 \quad \text{and} \quad E_b I_b \, \partial^2 \hat{w} / \partial \hat{x}^2 = 0 \quad \text{at} \quad \hat{x} = 0 \text{ and } \ell, \tag{2}$$

where $\hat{x}$ is the space co-ordinate along the horizontal projection of the centerline of the arch and $\hat{t}$ is the dimensional time; $\hat{\psi}$ and $\hat{w}$ indicate the initial rest configuration and the dynamic deflection measured from the rest configuration, respectively; ℓ is the span of the beam; ρ_b is the mass density; E_b is Young's modulus; A_b and I_b are the area and the moment of inertia of the cross-section, respectively; $\hat{c}$ is the viscous damping coefficient; $\hat{F}$ is the applied transverse load; and $\hat{U}$ indicates, at this stage, a general control input. Both ends of the beam are hinged whereby both the vertical and horizontal displacement components are restrained to be zero.

The equation of motion in the transverse direction, Eq. (1), is obtained after statically condensing the balance equation in the longitudinal direction. The longitudinal static condensation leads to the following expression for the axial force $\hat{N}$:

$$\hat{N}(\hat{x}, \hat{t}) = EA \left[\frac{\partial \hat{u}}{\partial \hat{x}} + \frac{\mathrm{d}\hat{\psi}}{\mathrm{d}\hat{x}} \frac{\partial \hat{w}}{\partial \hat{x}} + \frac{1}{2} \left(\frac{\partial \hat{w}}{\partial \hat{x}} \right)^2 \right],$$

and to the longitudinal displacement field in the form

$$\hat{u}(\hat{x}, \hat{t}) = \frac{\hat{x}}{\ell} \int_0^\ell \left[\frac{\mathrm{d}\hat{\psi}}{\mathrm{d}\hat{x}} \frac{\partial \hat{w}}{\partial \hat{x}} + \frac{1}{2} \left(\frac{\partial \hat{w}}{\partial \hat{x}} \right)^2 \right] \mathrm{d}x - \int_0^{\hat{x}} \left[\frac{\mathrm{d}\hat{\psi}}{\mathrm{d}\hat{x}} \frac{\partial \hat{w}}{\partial \hat{x}} + \frac{1}{2} \left(\frac{\partial \hat{w}}{\partial \hat{x}} \right)^2 \right] \mathrm{d}x.$$

The adopted mechanical model, based on linearized curvature, on a linear constitutive law relating bending moment and curvature, and on non-linear extension of the centerline, describes reasonably well the system behavior provided that the beam is sufficiently shallow and slender (the ratio between the thickness and radius of curvature is much smaller than unity). In this case, the mentioned decoupling between the longitudinal and transverse dynamics allows to solve for the transverse problem described by Eqs. (1)–(2) which is governed by quadratic (due to the moderate initial curvature) and cubic non-linearities (due to the axis extension). Inertia non-linearities do not appear because the longitudinal inertia is neglected. Further, the bending curvature has been linearized because moderately large deflections and small dynamic rotations are assumed.

The actuation is provided by two piezoceramic actuators mounted at given locations denoted by $\hat{x}_k$ (i.e., co-ordinate of the midspan axis of the piezoceramic patch) for the kth actuator of length ℓ_k. The ensuing control actions enter the equations of motion in the form [13]

$$\hat{U}(\hat{x},\hat{t}) = \sum_{k=1}^{2} \widehat{\mathscr{M}}_k(\hat{t}) \left[\frac{\mathrm{d}^2 \mathrm{H}(\hat{x}-\hat{x}_k^-)}{\mathrm{d}\hat{x}^2} - \frac{\mathrm{d}^2 \mathrm{H}(\hat{x}-\hat{x}_k^+)}{\mathrm{d}\hat{x}^2} \right], \tag{3}$$

where $\hat{x}_k^{\mp} = \hat{x}_k \mp \ell_k/2$ and H denotes the Heaviside unit-step function. In Eq. (3), $\widehat{\mathscr{M}}_k(\hat{t})$ is the time-varying amplitude of the bending moments delivered by the piezo actuators and expressed, in turn, as [13]

$$\widehat{\mathscr{M}}_k(\hat{t}) = \tfrac{1}{2} E_c w_c d_{31} (h_b + h_c) \hat{V}(\hat{t}), \tag{4}$$

where w_c and h_c are the width and thickness of the piezoceramic cross-section, respectively; h_b is the thickness of the beam; d_{31} and E_c are the transverse charge constant and Young's modulus of the piezoelectric material, respectively; and $\hat{V}(\hat{t})$ is the applied time-varying voltage.

A suitable non-dimensionalization of the governing equations yields the associated non-dimensional form as

$$\begin{aligned} &\frac{\partial^2 w}{\partial t^2} + \frac{\partial^4 w}{\partial x^4} - \frac{\mathrm{d}^2\psi}{\mathrm{d}x^2} \int_0^1 \frac{\mathrm{d}\psi}{\mathrm{d}x} \frac{\partial w}{\partial x}\,\mathrm{d}x - \frac{\partial^2 w}{\partial x^2} \int_0^1 \frac{\mathrm{d}\psi}{\mathrm{d}x} \frac{\partial w}{\partial x}\,\mathrm{d}x \\ &\quad - \frac{1}{2} \frac{\mathrm{d}^2\psi}{\mathrm{d}x^2} \int_0^1 \left(\frac{\partial w}{\partial x}\right)^2 \mathrm{d}x - \frac{1}{2} \frac{\partial^2 w}{\partial x^2} \int_0^1 \left(\frac{\partial w}{\partial x}\right)^2 \mathrm{d}x \\ &\quad = \varepsilon^{v_1} F(x,t) - \varepsilon^{v_2} c \frac{\partial w}{\partial t} + \varepsilon^{v_3} \sum_{k=1}^{2} \mathscr{M}_k(t) \left[\frac{\mathrm{d}^2 \mathrm{H}(x-x_k^-)}{\mathrm{d}x^2} - \frac{\mathrm{d}^2 \mathrm{H}(x-x_k^+)}{\mathrm{d}x^2} \right], \end{aligned} \tag{5}$$

with boundary conditions

$$w = 0 \quad \text{and} \quad \partial^2 w/\partial x^2 = 0 \quad \text{at} \quad x = 0 \text{ and } 1, \tag{6}$$

where $\hat{x}/x = \ell$, $\hat{w}/w = \hat{\psi}/\psi = r_b = \sqrt{I_b/A_b}$, $t/\hat{t} = \omega_b = \sqrt{E_b I_b/(\rho_b A_b \ell^4)}$ and ε indicates a small dimensionless number (i.e., $\varepsilon \ll 1$) used as an ordering parameter.

The non-dimensional parameters are defined as

$$\varepsilon^{v_1} F = (\ell^4/E_b I_b r_b)\hat{F}, \quad \varepsilon^{v_2} c = \ell^2/\sqrt{\rho_b A_b E_b I_b}\,\hat{c}, \quad \text{and } \varepsilon^{v_3} \mathscr{M}_i = \ell^2/(E_b I_b r_b^2)\widehat{\mathscr{M}}_i.$$

The initial shape of the beam is assumed in the form of a half-sinusoidal shape, namely, $\psi = b \sin \pi x$. Then, the eigenvalue problem governing the undamped unforced vibrations around

the initial configuration ψ is cast in the form

$$\frac{\partial^2 w}{\partial t^2} + \mathscr{L} w = \frac{\partial^2 w}{\partial t^2} + \frac{\partial^4 w}{\partial x^4} - \frac{\mathrm{d}^2 \psi}{\mathrm{d}x^2} \int_0^1 \frac{\mathrm{d}\psi}{\mathrm{d}x} \frac{\partial w}{\partial x} \mathrm{d}x = 0, \tag{7}$$

with the associated boundary conditions. Because the non-dimensional inertia is unitary, the eigenmodes are normalized in the standard form

$$\int_0^1 \phi_k^2 \mathrm{d}x = \langle \phi_k \phi_k \rangle = 1,$$

and are expressed as $\phi_k = \sqrt{2} \sin k\pi x$ with the associated circular frequencies $\omega_1 = \pi^2 \sqrt{1 + b^2/2}$ and $\omega_k = k^2 \pi^2$, for $k \geqslant 2$.

As reported in Ref. [14], hinged–hinged initially imperfect beams may possess internal resonances depending on the non-dimensional amplitude of the initial imperfection. Namely, a two–to–one internal resonance between the first and second modes occurs when $b \approx 3\sqrt{14}$. Moreover, one–to–one internal resonances between the first and second modes and between the first and third modes may be activated at the crossover points when b is near $\sqrt{30}$ and $4\sqrt{10}$, respectively. Prediction of the possible modal interactions in the beam is important to single out the conditions when the proposed control method would be ineffective. In fact, as it is illustrated in the next section, the control strategy is designed to reduce, within an acceptable level, the primary resonance of the second mode when this mode is away from internal resonances (i.e., for proper ranges of the initial imperfection amplitude).

3. Closed-loop control strategy: a perturbation approach

In this section, the non-linear control strategy is developed employing a perturbation approach [8–10]. The method of multiple scales [15] is used to attack directly the governing equations of motion and boundary conditions instead of treating finite degree-of-freedom discretized versions because it has been shown that treatment of a discretized set of distributed-parameter systems with quadratic and cubic non-linearities may lead to erroneous quantitative and, in some cases, qualitative results [16]. Therefore, the problem of order reduction is overcome along with other insidious drawbacks as spillover effects that need to be considered when designing control schemes for distributed-parameter systems.

The responses of the system to a primary resonance of the second mode are constructed when this mode does not interact with any other mode. The disturbance is $F(x,t) = f(x) \cos \Omega t$ with $\Omega = \hat{\Omega}/\omega_b \approx \omega_2$ and $\langle \phi_2(x) f(x) \rangle = \int_0^1 \phi_2(x) f(x) = D \neq 0$. At the same time, the system is subjected to a piezo-actuator control input which will be designed to maximize the reduction of the primary resonance vibrations.

To impart a purely symmetric input to the system, a symmetrical controller arrangement is necessary; in other words, it is required that the piezoceramic patches be placed symmetrically with respect to the beam midspan plane and be driven symmetrically. This entails that one piezo-actuator driver only is needed (Fig. 1). In particular, two equal piezoceramic patches ($\ell_1 = \ell_2$) are

attached to the beam surface so that $x_1 + x_2 = 1$ and $\mathscr{M}_1 = \mathscr{M}_2 = \mathscr{M}$. On account of Eq. (4), the dimensional piezomoment becomes

$$\widehat{\mathscr{M}}(\hat{t}) = \tfrac{1}{2} E_c w_c d_{31} (h_b + h_c) \hat{k}_c \hat{w}(\hat{x}_c, \hat{t}) \hat{v}(\hat{x}_c, \hat{t}),$$

whereas its non-dimensional counterpart is $M(t) = k_c w(x_c, t) v(x_c, t)$, where

$$k_c = \frac{1}{2} \frac{E_c w_c (h_b + h_c)}{\sqrt{E_b I_b \rho_b A_b}} d_{31} \hat{k}_c. \tag{8}$$

The control signal (i.e., the applied voltage) is assumed as a quadratic law of the form

$$\hat{V}(t) = \hat{k}_c \hat{w}(\hat{x}_c, \hat{t}) \hat{v}(\hat{x}_c, \hat{t}), \tag{9}$$

where $\hat{v} = \dot{\hat{w}}$ denotes the beam velocity field and $\hat{k}_c$ is the control gain. In Eq. (9), $\hat{x}_c$ indicates the co-ordinate of the reference point of the beam where the displacement and velocity are sensed to be fed back to the controller. The rationale behind this choice is the following. A preliminary direct perturbation expansion of the system dynamics suggests that the assumed quadratic control law (9) possesses the potential for producing appropriate resonant terms at third order where the external primary resonance effects are manifested. In fact, denoting with w_i and v_i the displacement and velocity at the ith order, respectively, it is, at first order, $w_1 \propto A \exp(\mathrm{i}\omega_2 t)$ and $v_1 \propto \mathrm{i}\omega_2 A \exp(\mathrm{i}\omega_2 t)$ whereas, at second order, part of the displacement is $\propto \mathrm{i}\omega_2 A^2 \exp(2\mathrm{i}\omega_2 t)$ where A indicates the complex-valued amplitude of the response at the system natural frequency (i is the imaginary unit). Consequently, the third-order structural non-linear forces $G_2(w_1, w_2)$ (G_2 is the operator governing the quadratic forces) are such to create terms $\propto \mathrm{i}\omega_2 A^2 \bar{A}$ where the bar denotes the complex conjugate. Because the control-induced force has the same phase as that of the damping force $\propto 2\mathrm{i}\omega_2 \mu A \exp(\mathrm{i}\omega_2 t)$, it is expected to act as a non-linear damping force.

In the next section, the perturbation treatment of the system dynamics with the controls is shown and discussed in detail.

3.1. Perturbation analysis

As typical for primary resonances, a third-order uniform expansion of the solutions of Eqs. (5) and (6) is determined. When the amplitude of the initial imperfection is of order one (i.e., $b = O(1)$), then all the coefficients of the linear and non-linear terms in the governing equation of motion are $O(1)$. Consequently, a third-order uniform expansion for the deflection and the associated velocity is sought in the form

$$w(x,t) \approx \sum_{k=1}^{3} \varepsilon^k w_k(x, T_0, T_2), \quad v(x,t) \approx \sum_{k=1}^{3} \varepsilon^k v_k(x, T_0, T_2), \tag{10}$$

where $T_0 = t$ is the fast scale associated with variations occurring at the frequency of the second mode, and $T_2 = \varepsilon^2 t$ is the stretched time scale governing the non-linear slow variations. The small dimensionless parameter ε is the same parameter introduced in the non-dimensional equation of motion as ordering parameter.

The solution is not assumed to depend on the scale $T_1 = \varepsilon t$ because resonant terms are produced by the external disturbance, control input and structural non-linearities at third order only. Consequently, the first derivative with respect to time can be expressed as $\partial/\partial t =$

$D_0 + \varepsilon^2 D_2 + \cdots$ where $D_n = \partial/\partial T_n$. Further, the nearness of the primary resonance is expressed introducing a detuning parameter σ such that $\Omega = \omega_2 + \varepsilon^2\sigma$ with $\sigma = O(1)$.

Because the beam is excited via an external primary resonance, the excitation and damping are ordered by letting $v_1 = 3$ and $v_2 = 2$ so that the damping, excitation and non-linear resonant terms balance each other at third order. According to previous comments, the control input governed by the quadratic law (9) is deliberately chosen to appear at second order by putting $v_3 = 0$ and assuming $k_c = O(1)$.

Substituting Eq. (10) into the system of first-order (in time) equations of motion and boundary conditions, using the independence of the time scales, and equating coefficients of like powers of ε yields

order ε

$$D_0 w_1 - v_1 = 0, \quad D_0 v_1 + \mathscr{L} w_1 = 0. \tag{11, 12}$$

order ε^2

$$D_0 w_2 - v_2 = 0, \tag{13}$$

$$\begin{aligned} D_0 v_2 + \mathscr{L} w_2 = {} & \frac{\partial^2 w_1}{\partial x^2} \int_0^1 \frac{\mathrm{d}\psi}{\mathrm{d}x} \frac{\partial w_1}{\partial x} \mathrm{d}x + \frac{1}{2} \frac{\mathrm{d}^2\psi}{\mathrm{d}x^2} \int_0^1 \left(\frac{\partial w_1}{\partial x}\right)^2 \mathrm{d}x \\ & + k_c w_1(x_c, T_0, T_2) v_1(x_c, T_0, T_2) \sum_{k=1}^{2} \left[\frac{\mathrm{d}^2 \mathrm{H}(x - x_k^-)}{\mathrm{d}x^2} - \frac{\mathrm{d}^2 \mathrm{H}(x - x_k^+)}{\mathrm{d}x^2} \right]. \end{aligned} \tag{14}$$

order ε^3

$$D_0 w_3 - v_3 = -D_2 w_1, \tag{15}$$

$$\begin{aligned} D_0 v_3 + \mathscr{L} w_3 = {} & - D_2 v_1 + \frac{\partial^2 w_1}{\partial x^2} \int_0^1 \frac{\mathrm{d}\psi}{\mathrm{d}x} \frac{\partial w_2}{\partial x} \mathrm{d}x + \frac{\partial^2 w_2}{\partial x^2} \int_0^1 \frac{\mathrm{d}\psi}{\mathrm{d}x} \frac{\partial w_1}{\partial x} \mathrm{d}x \\ & + \frac{\mathrm{d}^2\psi}{\mathrm{d}x^2} \int_0^1 \frac{\partial w_1}{\partial x} \frac{\partial w_2}{\partial x} \mathrm{d}x + \frac{1}{2} \frac{\partial^2 w_1}{\partial x^2} \int_0^1 \left(\frac{\partial w_1}{\partial x}\right)^2 \mathrm{d}x \\ & + k_c [w_1(x_c, T_0, T_2) v_2(x_c, T_0, T_2) + w_2(x_c, T_0, T_2) v_1(x_c, T_0, T_2)] \\ & \times \sum_{k=1}^{2} \left[\frac{\mathrm{d}^2 \mathrm{H}(x - x_k^-)}{\mathrm{d}x^2} - \frac{\mathrm{d}^2 \mathrm{H}(x - x_k^+)}{\mathrm{d}x^2} \right] - 2\mu v_1 + \frac{1}{2} f(x)(\mathrm{e}^{\mathrm{i}\Omega T_0} + cc), \end{aligned} \tag{16}$$

where $c = 2\mu$ and cc indicates the complex conjugate of the preceding terms. The boundary conditions at all orders are given by Eq. (6).

Because the second mode is directly excited by the primary-resonance disturbance and, indirectly, by the control input and because this mode cannot interact with any other mode (for the absence of internal resonances), the solution at order ε is assumed as

$$w_1 = A(T_2)\mathrm{e}^{\mathrm{i}\omega_2 T_0} \phi_2(x) + \bar{A}(T_2)\mathrm{e}^{-\mathrm{i}\omega_2 T_0} \phi_2(x). \tag{17}$$

Substituting Eq. (17) and $v_1 = D_0 w_1$ into the second-order problem, Eqs. (13) and (14), yields

$$D_0 w_2 - v_2 = 0. \tag{18}$$

$$D_0 v_2 + \mathscr{L} w_2 = (A^2 \mathrm{e}^{2\mathrm{i}\omega_2 T_0} + A\bar{A})\psi'' \int_0^1 (\phi_2')^2 \mathrm{d}x + \mathrm{i}\omega_2 k_c \phi_{2c}^2 A^2 \mathrm{e}^{2\mathrm{i}\omega_2 T_0} \times \sum_{k=1}^{2} [\mathrm{H}''(x - x_k^-) - \mathrm{H}''(x - x_k^+)] + cc, \tag{19}$$

where the prime indicates differentiation with respect to x and $\phi_{2c} = \phi_2(x_c)$ is the value attained by the second mode shape at x_c.

Then, the second-order solution can be expressed as

$$w_2 = A^2 \mathrm{e}^{2\mathrm{i}\omega_2 T_0} \chi_1(x) + A\bar{A}\chi_2(x) + \mathrm{i}\omega_2 k_c \phi_{2c}^2 A^2 \mathrm{e}^{2\mathrm{i}\omega_2 T_0} \mathscr{U}_c(x) + cc, \tag{20}$$

$$v_2 = 2\mathrm{i}\omega_2 A^2 \mathrm{e}^{2\mathrm{i}\omega_2 T_0} \chi_1(x) - 2\omega_2^2 k_c \phi_{2c}^2 A^2 \mathrm{e}^{2\mathrm{i}\omega_2 T_0} \mathscr{U}_c(x) + cc, \tag{21}$$

where the functions χ_1, χ_2, and $\mathscr{U}_c$ are solutions of the boundary-value problems:

$$\mathscr{L}\chi_1 - 4\omega_2^2 \chi_1 = \tfrac{1}{2}\psi'' \langle \phi_2' \phi_2' \rangle = -4b\pi^4 \sin \pi x. \quad \mathscr{L}\chi_2 = -4b\pi^4 \sin \pi x, \tag{22, 23}$$

$$\mathscr{L}\mathscr{U}_c - 4\omega_2^2 \mathscr{U}_c = \sum_{k=1}^{2} [\mathrm{H}''(x - x_k^-) - \mathrm{H}''(x - x_k^+)], \tag{24}$$

with the boundary conditions (6).

The solutions of the first two boundary-value problems are obtained in the form

$$\chi_1(x) = -\frac{4b}{b^2 - 126} \sin \pi x \quad \text{and} \quad \chi_2(x) = -\frac{4b}{b^2 + 2} \sin \pi x. \tag{25}$$

On the other hand, using the modal expansion method, the function $\mathscr{U}_c$ can be expressed as an infinite series of the symmetric eigenmodes in the form

$$\mathscr{U}_c(x) = \sum_{k=0}^{\infty} \frac{m_{2k+1}}{\omega_{2k+1}^2 - 4\omega_2^2} \phi_{2k+1}(x), \tag{26}$$

where

$$m_j = \phi_j'(x_1^+) - \phi_j'(x_1^-) + \phi_j'(x_2^+) - \phi_j'(x_2^-) \tag{27}$$

is the jth modal force produced by unitary moments delivered by the two actuators. The second-order shape functions are shown in Fig. 2 when $b = 3.5$, $\ell_1 = \ell_2 = \ell/15$, $x_1 = 1/4$, and $x_2 = 3/4$. Four terms only in the series (26) were sufficient for convergence.

Substituting the second-order solution into the third-order problem, and enforcing solvability of the resulting inhomogeneous partial-differential problem, yields the modulation equation

$$2\mathrm{i}\omega_2(D_2 A + \mu A) = \mathrm{i}\omega_2 k_c \mu_c A^2 \bar{A} + \alpha A^2 \bar{A} + \tfrac{1}{2} D \mathrm{e}^{\mathrm{i}\sigma T_2}, \tag{28}$$

where μ_c is the coefficient of the non-linear *control-induced damping* term, α is the *effective non-linearity coefficient* and $D = \langle f(x)\phi_2(x) \rangle$ is the *disturbance modal amplitude*. The coefficient μ_c is expressed as

$$\mu_c = \phi_{2c}^2 \langle \phi_2'' \phi_2 \rangle \langle \psi' U_c' \rangle = -8\sqrt{2} \frac{b}{b^2 - 126} (\sin 2\pi x_c)^2 m_1. \tag{29}$$

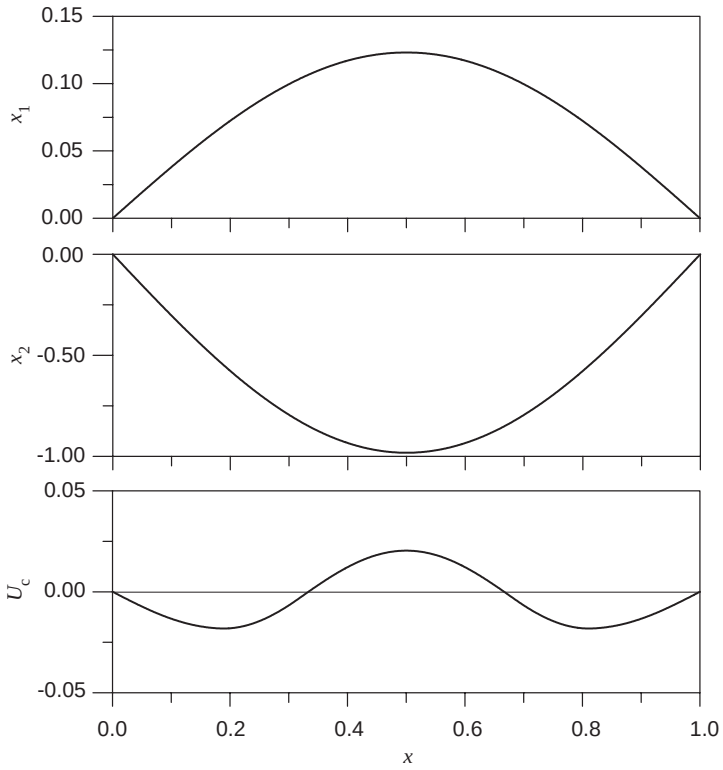

Fig. 2. The second-order shape functions χ_1, χ_2, and U_c when $b = 3.5$, $\ell_1 = \ell_2 = \ell/15$, $x_1 = 1/4$, and $x_2 = 3/4$.

On the other hand, the effective non-linearity coefficient is expressed as

$$\alpha = \langle \phi_2 \phi_2'' \rangle \left[2\langle \psi' \chi_2' \rangle + \langle \psi' \chi_1' \rangle + \frac{3}{2} \langle \phi_2' \phi_2' \rangle \right] = 16\pi^4 \frac{378 + 61b^2}{(b^2 + 2)(b^2 - 126)}. \tag{30}$$

In the next section, the steady-state responses of the beam with and without controls are put in real form and their meaningful characteristics are discussed.

3.2. System responses

First, the slow dynamics are discussed by considering the modulation equations. These equations describe the envelope of the fast oscillations at the system natural frequency; the envelope is determined by the interaction of the excitation, damping, and control-induced forces with the resonant parts of the non-linear restoring forces.

To transform the complex-valued modulation equation into real-valued equations for the amplitude and phase, the polar transformation $A = 1/2\, a \exp(\mathrm{i}\beta) \exp(\mathrm{i}(\sigma t - \gamma))$ is substituted into Eq. (28) thereby yielding

$$\dot{a} = -\mu a + k_c \mu_c a^3 + (D/2\omega_2) \sin\gamma, \quad \dot{\gamma} = \sigma + (\alpha/8\omega_2) a^2 + (D/2\omega_2 a) \cos\gamma. \tag{31, 32}$$

The steady-state responses of the controlled beam are obtained as the fixed points of the modulation equations (31) and (32) (i.e., $\dot{a} = \dot{\gamma} = 0$). As a result, periodic responses of the controlled beam are governed by the frequency-response equation

$$\sigma = -(\alpha/8\omega_2)a^2 \pm \sqrt{D^2/(4\omega_2^2 a^2) - (\mu - k_c\mu_c a^2)^2} \tag{33}$$

and the expression for the phase

$$\tan\gamma = \mp\mu - k_c\mu_c a^2 / \sqrt{D^2/(4\omega_2^2 a^2) - (\mu - k_c\mu_c a^2)^2}. \tag{34}$$

Inspection of Eqs. (30) and (33) allows one to conclude that, when $b < 3\sqrt{14}$, $\alpha < 0$. Accounting for this and the fact that the non-linear free oscillation frequency is given by

$$\omega_{2N} = \omega_2 - (\alpha/8\omega_2)a^2,$$

the non-linear free oscillation frequency of the mode increases with the oscillation amplitude and the mode is a hardening mode.

On the other hand, when $b > 3\sqrt{14}$, $\alpha > 0$; the non-linear free oscillation frequency decreases with the oscillation amplitude, hence, the mode is a softening mode. When $b = 3\sqrt{14}$, a two-to-one internal resonance between the first two modes is activated and the present asymptotic expansion breaks down. In this case, an expansion accounting for the two-mode interaction is needed to calculate the actual effective non-linearity coefficient [14].

Using Eqs. (17), (20), the polar transformation for A, and the frequency detuning $\Omega = \omega_2 + \varepsilon^2\sigma$, the deflection of the controlled beam is expressed as

$$\begin{aligned} w(x,t) = {} & a\cos(\Omega t - \gamma)\phi_2(x) + \tfrac{1}{2}a^2[\cos 2(\Omega t - \gamma)\chi_1(x) + \chi_2(x)] \\ & - \tfrac{1}{2}k_c\omega_2\phi_{2c}^2 a^2 \sin 2(\Omega t - \gamma)\mathscr{W}_c(x) + \cdots. \end{aligned} \tag{35}$$

where a and γ are governed, at steady state, by Eqs. (33) and (34), respectively.

Clearly, the frequency response equation and the phase of the uncontrolled beam can be obtained from Eqs. (33) and (34) putting $k_c = 0$ into them. The ensuing frequency-response equation of the uncontrolled resonance is

$$\sigma = -(\alpha/8\omega_2)a^2 \pm \sqrt{D^2/(4\omega_2^2 a^2 - \mu^2)}, \tag{36}$$

whereas the phase is given by

$$\tan\gamma = \mp\mu / \sqrt{D^2/(4\omega_2^2 a^2) - \mu^2}. \tag{37}$$

Similarly, the deflection of the uncontrolled beam is expressed as

$$w(x,t) = a\cos(\Omega t - \gamma)\phi_2(x) + \tfrac{1}{2}a^2[\cos 2(\Omega t - \gamma)\chi_1(x) + \chi_2(x)] + \cdots, \tag{38}$$

where a and γ are governed by Eqs. (36) and (37), respectively.

In the next section, the performance of the non-linear control strategy is investigated.

4. Control performance

It is clear from Eq. (33) that the amplitude of the controlled response is reduced as a result of the non-linear quadratic damping term $k_c\mu_c a^2$ which increases the overall system damping, more effectively when $\mu_c<0$, assuming that k_c is strictly positive. On account of Eq. (29) and of the fact that $m_1<0$, this coefficient is negative when $b<3\sqrt{14}$ and is positive when $b>3\sqrt{14}$. Further, as expected, μ_c depends on x_c and m_1. The dependence on x_c allows to conclude that $|\mu_c|$ is maximum when $x_c=1/4$ or $3/4$. On the other hand, $|\mu_c|$ grows linearly with m_1 which, in turn, depends on the location and length of the actuators. However, often the actuator positions are physically constrained.

In the proposed control architecture, because the actuation is provided by two equal piezo actuators attached at one-fourth and three-fourth of the beam span and whose length is one-fifteenth of the beam span (i.e., $x_1=1/4$, $x_2=3/4$, and $\ell_1=\ell_2=\ell/15$), it is

$$\mu_c=-\frac{16\pi b}{b^2-126}(\cos\pi x_1^+-\cos\pi x_1^-+\cos\pi x_2^+-\cos\pi x_2^-). \tag{39}$$

To evaluate the control performance, among a variety of possible cost functions, the selected cost function is the maximum amplitude of the harmonic response component at the excitation frequency attained by the beam when the frequency is varied near resonance. Of course, this cost is calculated based on steady-state rather than on transient effects. Hence, it reflects the cost predicted over long periods of operation where transients die out. Moreover, as alternative cost function, the maximum of the integral of the squared deflection over the span attained in one excitation cycle was also computed so as to capture directly higher-order effects. That is,

$$J=\max_{t\in[0,T_c]}\left\{\int_0^1 w(x,t;a_c)^2\,\mathrm{d}x\right\}, \tag{40}$$

where T_c is the period of oscillation and a_c is the maximum stable value of the amplitude a at the disturbance frequency. For the first cost function, a closed-form expression was obtained in the form

$$a_c=\frac{-26^{2/3}\mu\omega_2^{2/3}+6^{1/3}(9D\sqrt{|\mu_c|k_c}+\sqrt{81D^2|\mu_c|k_c+48\mu^3\omega_2^2})^{2/3}}{6\sqrt{|\mu_c|k_c}\omega_2^{1/3}(9D\sqrt{|\mu_c|k_c}+\sqrt{81D^2|\mu_c|k_c+48\mu^3\omega_2^2})^{1/3}}. \tag{41}$$

The maximum amplitude of the system uncontrolled response is $a_{uc}=D/(2\omega_2\mu)$. Accordingly, the control performance can be quantified calculating the following performance function $\Gamma=100\times(a_{uc}-a_c)/a_{uc}$ which expresses the percent relative peak amplitude reduction. Because μ_c is fixed once the number of actuators, their dimensions, and positions are chosen, the performance function depends only on the control gain k_c that can be varied. In Fig. 3, variation of the performance function Γ with the control gain k_c is shown. Interestingly, this function exhibits a rather sharp increase in a small range of gains below 1 whereas it shows a saturation-type behavior with a nearly flat trend for higher gains. More specifically, a 60% reduction is attained with a gain slightly below 0.5 whereas the reduction becomes higher than 70% when $k_c=1$. This result makes the proposed control strategy effective and feasible because relatively small control efforts are needed to obtain good control performances. In Table 1, the peak controlled response

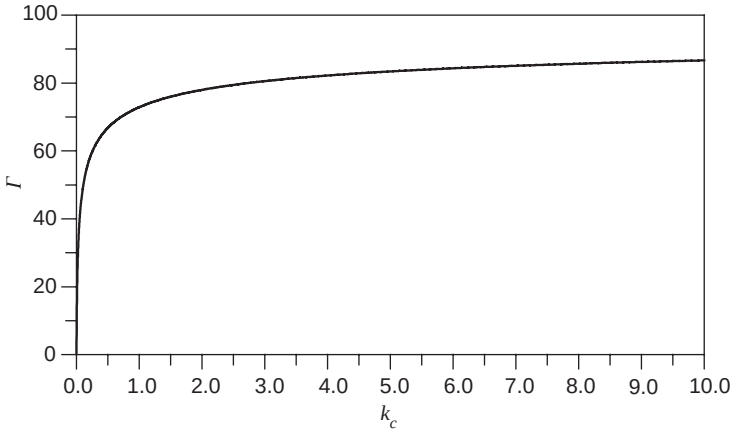

Fig. 3. Variation of the control performance function Γ with the control gain k_c when $b = 3.5$, $D = 0.5$, $\mu = 0.01$, $\ell_1 = \ell_2 = \ell/15$, $x_1 = 1/4$, and $x_2 = 3/4$.

Table 1
Control performance

k_c	a_c	$\Gamma = (a_{uc} - a_c)/a_{uc}\%$	$(J_{uc} - J_c)/J_{uc}\%$
1	0.172	72.9	92.9
5	0.105	83.4	97.3
7.5	0.093	85.4	97.9
10	0.084	86.7	98.3

amplitude a_c is reported along with the performance function calculated using either the cost function based on the peak amplitude or that based on the maximum of the integral of the squared steady-state beam deflection. For the uncontrolled beam when $b = 3.5$, $D = 0.5$, and $\mu = 0.01$, the following quantities were calculated: $a_{uc} = 0.633$, $\sigma_{uc} = 1.374$ (point A in Figs. 4 and 5), and $J_{uc} = 0.416$.

Indeed, it is critical to ascertain that the controlled responses are stable in the overall considered frequency range. To this end, the eigenvalues of the Jacobian of Eqs. (31) and (32) were calculated. The outcomes indicated that the steady-state responses are either stable foci or stable nodes. In Fig. 4, some frequency-response curves of the uncontrolled and controlled beam are shown. In this figure and henceforth, thick (dashed) lines denote stable (unstable) responses.

To gain more insight into the effects of the control action onto the beam dynamics, in Fig. 5, variation of the phase of the steady-state system response with the frequency detuning is shown. The uncontrolled response exhibits the well-known phase distortion effect exerted by the nonlinear resonance. The control action, instead, increasing the system damping, renders the phase behavior closer to that of a linear system although slightly distorted.

Finally, to show the overall effectiveness of the control strategy including the transient behavior, in Fig. 6, the time histories of the beam deflection at one-fourth of the beam span with

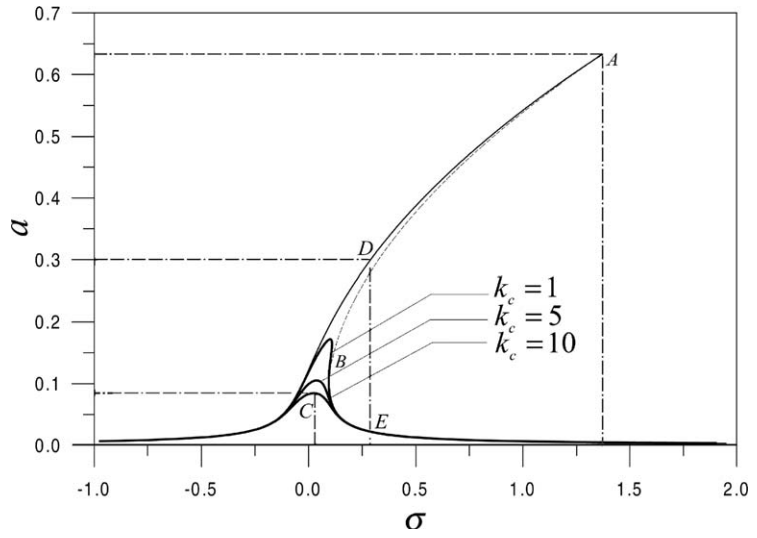

Fig. 4. Frequency-response curves of the uncontrolled and controlled beam for different control gains when $b = 3.5$, $D = 0.5$, $\mu = 0.01$, $\ell_1 = \ell_2 = \ell/15$, $x_1 = 1/4$, and $x_2 = 3/4$. Points A and B denote saddle-node bifurcations.

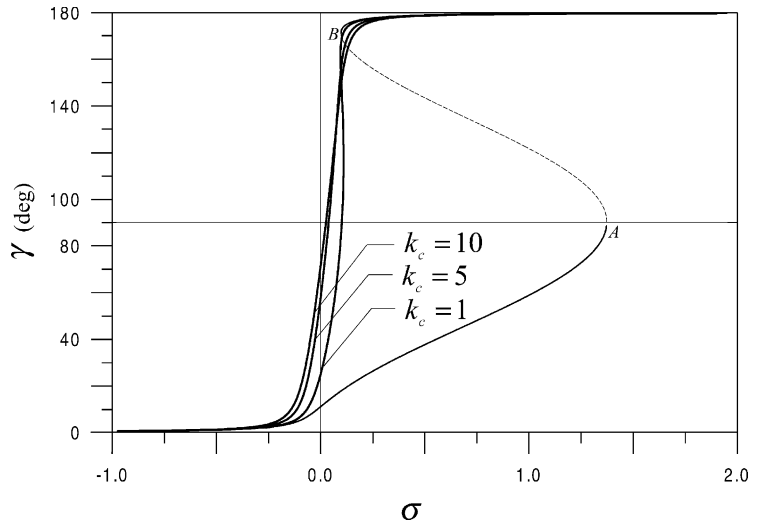

Fig. 5. Variation of the phase of the steady-state responses of the uncontrolled and controlled beam when $b = 3.5$, $D = 0.5$, $\mu = 0.01$, $\ell_1 = \ell_2 = \ell/15$, $x_1 = 1/4$, and $x_2 = 3/4$.

and without controls are compared when the excitation frequency detuning is $\sigma = 0.327$ and $k_c = 10$ (points D and E in Fig. 4). The initial conditions are $a(0) = 0.3$ and $\gamma(0) = -0.49$. These time histories have been obtained integrating numerically Eqs. (31) and (32) with $k_c = 0$ and using Eq. (38), for the uncontrolled case, and Eq. (35), for the controlled case, respectively. In addition,

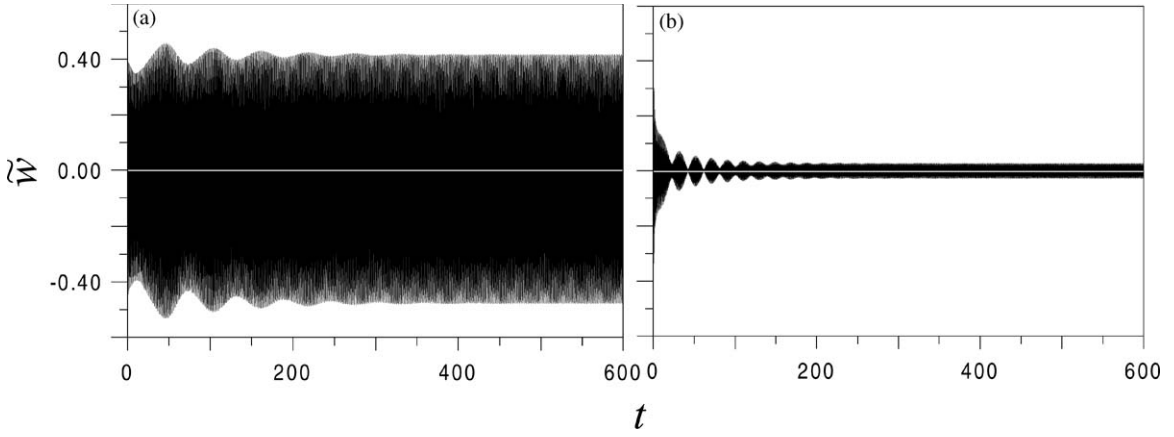

Fig. 6. Time histories of the beam deflection at $x = 1/4$: (a) uncontrolled and (b) controlled when $b = 3.5$, $D = 0.5$, $\sigma = 0.327$, $\mu = 0.01$, $\ell_1 = \ell_2 = \ell/15$, $x_1 = 1/4$, $x_2 = 3/4$, and $k_c = 10$.

the reduction of the overall beam deflection field is shown in Fig. 7 where there are reported the deflections of the beam in the uncontrolled (point A in Figs. 4 and 5) and controlled (point C in Fig. 4) cases at equally spaced discrete times in one excitation cycle. The response is reduced in the overall beam span by an order of magnitude.

5. Conclusions

In this paper, a closed-loop non-linear control method to reduce the flexural forced vibrations of a hinged–hinged initially imperfect beam has been investigated. The disturbance is involved in a primary resonance with the first antisymmetric mode of the beam. The basic idea relates to the fact that the non-collocated control action—bending moments imparted by two symmetrically placed piezo actuators—is designed intelligently so as to have control authority onto antisymmetric vibrations by exploiting the system non-linearities.

The fact that a non-linear controller with a symmetric input is shown to reduce also antisymmetric vibrations entails that the control capabilities have been expanded by exploitation of the structural non-linearities with respect to the linear theory. In fact, the same controller designed primarily to reduce symmetric oscillations may be used to reduce antisymmetric vibrations which, under some excitation conditions (e.g., as in suspension bridges), can be excited simultaneously with symmetric vibrations.

As a distinguishing feature, the design process of the control law has been based on use of a perturbation technique to facilitate understanding of the way the non-linear controller action can affect the resonant system dynamics. Furthermore, the analytical approximate responses of the beam, obtained with direct application of the method of multiple scales to the integral–partial differential equations of motion and boundary conditions, were used to investigate the overall features of the control method and the main technical conditions for its effectiveness. Along these lines, it was possible to obtain a closed-form expression of a representative cost function which

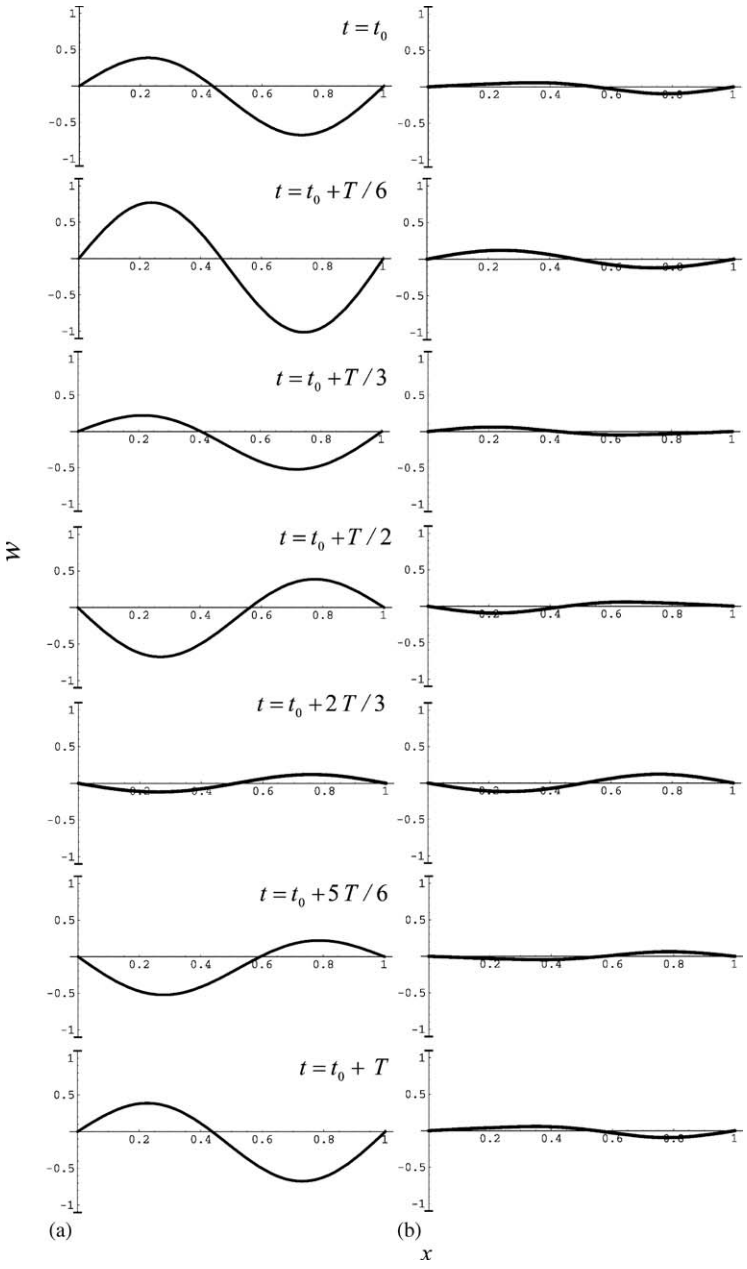

Fig. 7. Deflections of the beam in one excitation cycle (period T): (a) uncontrolled, $\sigma = 1.374$ and (b) controlled, $\sigma = 0.0245$ with parameters as listed for Fig. 3.

allowed to study the performance of the control method with respect to variations of the control gain. As a major outcome, for rather low gain values, the reduction in motion amplitude has been shown to be about 70% at resonance.

Acknowledgements

This work was partially sponsored under the *FY-2001 Gaikokujin Kenkyusha Program* and the *FY-2002 Short-Term Fellowship by the Japan Society for the Promotion of Science*, *N. S02721* at the University of Tsukuba, Japan.

References

[1] A.H. Nayfeh, D.T. Mook, *Nonlinear Oscillations*, Wiley-Interscience, New York, 1979.
[2] Y. Fujino, P. Warnitchai, B.M. Pacheco, Active stiffness control of cable vibration, *American Society of Mechanical Engineers, Journal of Applied Mechanics* 60 (1993) 948–953.
[3] V. Gattulli, M. Pasca, F. Vestroni, Nonlinear oscillations of a nonresonant cable under in-plane excitation with a longitudinal control, *Nonlinear Dynamics* 14 (1997) 139–156.
[4] S.S. Oueini, A.H. Nayfeh, J.R. Pratt, A nonlinear vibration absorber for flexible structures, *Nonlinear Dynamics* 15 (1998) 259–282.
[5] H. Yabuno, J. Kawazoe, N. Aoshima, Suppression of parametric resonance of a cantiliver beam by a pendulum-type vibration absorber, in: *Proceedings of the 17th Biennial ASME Conference on Mechanical Vibration and Noise*, Las Vegas, NV, 1999.
[6] H. Yabuno, S. Saigusa, N. Aoshima, Stabilization of the parametric resonance of a cantilever beam by bifurcation control with a piezoelectric actuator, *Nonlinear Dynamics* 26 (2001) 143–161.
[7] A. Maccari, Vibration control for the primary resonance of a cantilever beam by time delay state feedback, *Journal of Sound and Vibration* 259 (2003) 241–251.
[8] W. Lacarbonara, R.R. Soper, C.-M. Chin, Nonlinear vibration control of distributed-parameter systems: a perturbation approach, in: *Proceedings of the ASME Materials & Mechanics Conference*, Blacksburg, VA, 1999.
[9] W. Lacarbonara, C.M. Chin, R.R. Soper, Open-loop nonlinear vibration control of shallow arches via perturbation approach, *Journal of Applied Mechanics* 69 (2002) 325–334.
[10] R.R. Soper, W. Lacarbonara, C.M. Chin, A.H. Nayfeh, D.T. Mook, Open-loop resonance-cancellation control for a base-excited pendulum, *Journal of Vibration and Control* 7 (2001) 1265–1279.
[11] R. Kanda, H. Yabuno, W. Lacarbonara, N. Aoshima, Stabilization of the parametric resonance in a magnetically levitated body using a nonlinear pendulum-type vibration absorber, in: *Proceedings of the 9th International Conference on Sound and Vibration*, Orlando, FL, 2002.
[12] E. Mettler, Dynamic buckling, in: W. Flugge (Ed.), *Handbook of Engineering Mechanics*, McGraw-Hill, New York, 1962.
[13] J.L. Fanson, T.K. Caughey, Positive position feedback for large space structures, *American Institute of Aeronautics and Astronautics Journal* 28 (1990) 717–724.
[14] W. Lacarbonara, G. Rega, Resonant nonlinear normal modes of shallow one-dimensional structural systems. Part II: activation/orthogonality conditions, *International Journal of Non-Linear Mechanics* 38 (2003) 873–887.
[15] A.H. Nayfeh, *Introduction to Perturbation Techniques*, Wiley-Interscience, New York, 1981.
[16] W. Lacarbonara, A.H. Nayfeh, W. Kreider, Experimental validation of reduction methods for weakly nonlinear distributed-parameter systems: analysis of a buckled beam, *Nonlinear Dynamics* 17 (1998) 95–117.